
Article:
Gan, L.H., Wu, R., Tian, J.L. et al. (1 more author) (2016) An atlas of endohedral Sc2S cluster fullerenes. Physical Chemistry Chemical Physics, 19. pp. 419-425. ISSN 1463-9076

https://doi.org/10.1039/c6cp07370k

An atlas of endohedral Sc_2S cluster fullerenes

Li-Hua Gan*, Rui Wu, Jian-Lei Tian and Patrick W. Fowler*

School of Chemistry and Chemical Engineering, Southwest University, Chongqing, China 400715

Department of Chemistry, Sheffield University, Sheffield, S3 7HF, UK

E-mail: ganlh@swu.edu.cn; P.W.Fowler@sheffield.ac.uk

Abstract:

Structural identification is a difficult task in the study of metallofullerenes, but understanding of the mechanism of formation of these structures is a pre-requisite for new high-yield synthetic methods. Here, systematic density functional theory calculations demonstrate that metal sulfide fullerenes $Sc_2S@C_n$ have similar cage geometries from C_{70} to C_{84} and form a close-knit family of structures related by Endo-Kroto insertion/extrusion of C_2 units and Stone-Wales isomerization transformations. The stabilities predicted for favored isomers by DFT calculations are in good agreement with available experimental observations, have implications for the formation of metallofullerenes, and will aid structural identification from within the combinatorially vast pool of conceivable isomers.

Keywords: metallic sulfide cluster fullerenes; electron transfer; Stone-Wales rotation; Endo-Kroto C_2 insertion

1. Introduction

Endohedral metallofullerenes (EMFs) are closed cage-shaped molecules with encaged metal atoms or clusters [1, 2]. Since their first synthesis in macroscopic amounts [3], EMFs have attracted extensive interest from chemists, physicists and materials scientists. To date, more than two hundred EMFs have been characterized, including mono-metallofullerenes, dimetallofullerenes, trimetallofullerenes, and fullerenes incorporating clusters various kinds [4]. Amongst the EMFs, those in which the encapsuland is a metallic cluster have attracted attention because of their novel geometries and properties [5, 6]. However, as far as we are aware, the mechanism of formation of EMFs has not yet been clarified, even though so many EMFs have been reported. For small fullerenes, a recent theoretical study shows that C_2 insertion (by the Endo-Kroto mechanism) can facilitate the formation of larger fullerenes without additional Stone-Wales (S-W) rotations [7]. Where the cage is larger than C_{70}, direct C_2 insertion in classical isomers will form non-IPR (IPR = isolated pentagon rule [8]) isomers, which is not in agreement with experimental observations that all reported stable (neutral, bare) fullerenes are IPR-satisfying. Hence, C_2 insertion alone cannot account for the formation of fullerenes. Some post-insertion step, for which S-W rotation is the best candidate, is a necessary stage in the formation of fullerenes.

For endohedral metallic cluster fullerenes, formation processes may be similar to those for bare fullerenes, at least in terms of the cages involved, but they are likely to be affected by the presence of the additional participant. A pre-formed fullerene cage would almost certainly be broken by insertion of a metallic cluster into its interior, as the available windows, hexagonal, pentagonal or heptagonal faces, are small. It seems highly improbable that a metallic cluster will insert to form an EMF directly. Thus, reasonable formation paths would seem to require

growth or shrinkage of a cage with a cluster inside, or curling up to form fullerene cages with simultaneous encapsulation of a metal atom/cluster, as is consistent with molecular dynamics simulations [9].

Recent experiments show that non-classical fullerene cages with a heptagonal ring can also encapsulate metallic clusters [10], or can be captured as chlorofullerenes [11] from the carbon-arc plasma *in situ*. Theoretical studies show that heptagonal rings may play an important role in the formation of bare fullerenes [12, 13] and trimetallic nitride template fullerenes [14]. To predict the geometrical structures of some poorly characterized metallofullerenes and seek insight into their formation, it was decided to make a systematic study of classical and non-classical isomers $Sc_2S@C_n$ (n = 70-84). This was carried out with the help of an extended face-spiral algorithm for construction of cage candidates with small numbers of heptagonal faces. The results show that heptagon-including metallic sulfide fullerenes $Sc_2S@C_n$ are not competitive with classical $Sc_2S@C_n$ in terms of total energy. Interestingly, there are strong structural similarities amongst low-energy $Sc_2S@C_n$ isomers of equal and adjacent cage sizes. These similarities are given concrete form in terms of S-W isomerization and C_2 insertion/extrusion transformations. Our results provide clues to finding new metallofullerenes from within the tens of thousands of conceivable structural isomers. They also give potentially useful information on the formation mechanisms of EMFs.

2. Computational Details

The isomers to be considered are generated by an extension of the face-spiral algorithm to allow up to one heptagonal and 13 pentagonal faces [15]. This approach is known to be complete in the size range. The nomenclature and labelling of isomers follow the face-spiral algorithm. Briefly, classical isomers are labelled by their positions in the sequence of canonical spirals, and a superscript (1h) is used to indicate a non-classical isomer with one heptagon, with a number indicating its position in the spiral order for these cages. Topological coordinates [15] are used to provide initial cage structures, which are then optimized for charges 0, -2, –4 and -6, first at the semi-empirical PM3 level and, for a selection of the best cages at each charge, at the B3LYP/3-21G level. Based on the energy ranking for the optimized cages with charge -4, and some other favored isomers with different charges, the favored cages are used as parents to construct Sc_2S-based EMFs. The Sc_2S moiety is placed close to the geometric centre of the cage, and irrespective of the initial shape and atom ordering (Sc-S-Sc or S-Sc-Sc) optimizes to a structure where S lies between the two Sc centres; this is a simple consequence of the fact that the moiety donates electrons to the cage, generating electrostatic repulsion between the newly formed ionic Sc centres. The numbers of isomers considered by nuclearity are shown in S1. Geometrical optimizations are

performed at B3LYP/3-21G and then B3LYP/6-31G* levels on $Sc_2S@C_n$ with n from 70 to 84. All calculations are performed with Gaussian 09 software [16]. The results for the favored isomers are shown in Figure 1 and Table 1, and the optimized coordinates calculated for the isomers of lowest energy are provided in S2. In the optimized structures for the favoured isomers, the Sc-S-Sc angle varies between 140° and 180° in most cases, with $Sc_2S@C_{76}$:19151 having a much smaller angle of 108°. The linear Sc-S-Sc moieties are found in $Sc_2S@C_{74}$:13333 and $Sc_2S@C_{84}$:51591 (see coordinates in S2).

3. Results and discussion

Table 1 Numbers of pentagon adjacencies (N_{55}), relative energy (ΔE, kcal/mol), HOMO-LUMO gap (eV) and Sc-Sc distance (Å) for the lowest-energy isomers of $Sc_2S@C_n$.

Cage	N_{55}	ΔE	Gap	Sc-Sc	Cage	N_{55}	ΔE	Gap	Sc-Sc	Cage	N_{55}	ΔE	Gap	Sc-Sc
C_{70}:7892-C_2	2	0.0	1.84	3.597	C_{76}:19151-T_d	0	0.0	1.45	3.801	C_{82}:39715-Cs	0	0.0	1.72	4.073
C_{70}:7957-C_2	2	20.8	1.54	4.584	C_{76}:17490-C_s	2	11.3	1.32	4.546	C_{82}:39717-C3v	0	0.3	2.08	4.008
C_{70}:7924- C_1	2	20.9	1.35	4.241	C_{76}:19138-C_1	1	12.0	0.76	4.599	C_{82}^{1h}:155199(C1)	1	12.8	1.81	4.129
C_{72}:10528-C_s	2	0.0	1.85	4.225	C_{78}:24088-C_{2v}	2	0.0	1.76	4.207	C_{82}:39718-C2v	0	14.3	1.20	4.363
C_{72}:10616-C_s	2	13.9	1.93	4.425	C_{78}:24109-D_{3h}	0	1.7	0.97	4.485	C_{84}:51591-D2d	0	0.0	1.68	4.621
C_{72}:10530-C_1	2	19.1	1.66	3.979	C_{78}:24107-C_{2v}	0	3.7	1.53	4.168	C_{84}:51383-C1	1	10.4	1.90	4.447
C_{74}:13333-C_2	2	0.0	1.68	4.651	C_{80}:31923-D_{5h}	0	0.0	1.12	4.108	C_{84}:51580-C1	0	12.3	1.73	4.163
C_{74}:14246-D_{3h}	0	11.8	1.14	3.815	C_{80}:31922-C_{2v}	0	9.0	1.67	3.840					
C_{74}:14239-C_{2v}	2	11.9	1.21	4.157	C_{80}:31924-I_h	0	9.2	0.84	4.196					

Figure 1 shows the structures for the three most favored isomers for each of the eight formulas Sc_2S $@C_n$ with n = 70-84.

It is shown in Table 1 that the isomer of lowest energy isomer for $Sc_2S@C_{70}$ has a large HOMO-LUMO gap (1.84 eV) and parent cage, the non-IPR C_{70}:7892, with two pentagon adjacencies. The stability of this isomer is in good agreement with experimental results [17]. In fact, this cage has recently been shown to be the parent of a geometrically and electronically similar cluster Sc_2O [18]. The two isomers next in energy order are also classical, but lie more than 20 kcal mol^{-1} higher.

It is shown in Table 1 that $Sc_2S@C_{72}$:10528 is the first favored isomer in energy terms and has a large gap of 1.85 eV. The next most favored isomer is higher in energy by 13.9 kcal mol^{-1} than the first, which corresponds to an equilibrium fractional population of only 3% at 2000 K. This isomer and others of higher energy are unlikely to be isolated in significant yield. The isomer predicted to be most favored corresponds to experimental observations [19a] and recent theoretical results [19b]. The same parent cage is shared by the electronically

similar cluster Sc_2C_2 in the metallic carbide fullerene $Sc_2C_2@C_{72}$ [20], and the electronically and geometrically similar cluster Sc_2O in the metallic oxide fullerene $Sc_2O@C_{72}$ [21].

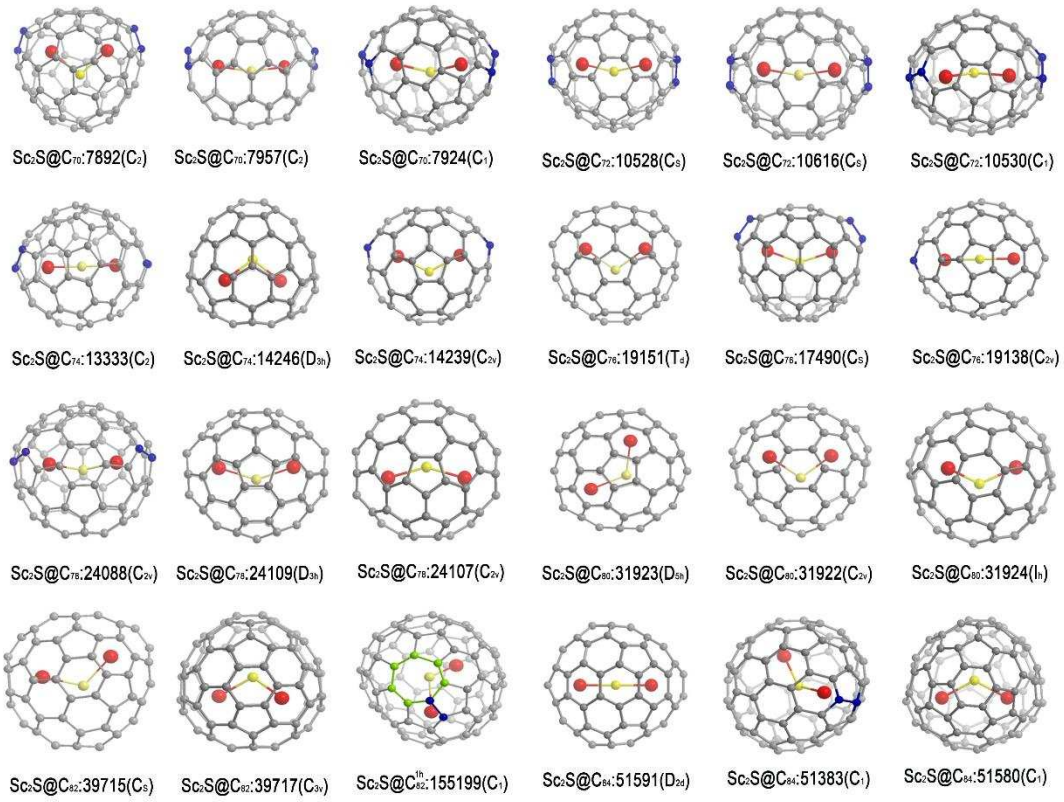

Fig. 1 Optimized structures of the three isomers of lowest energy for each $Sc_2S@C_n$ with n from 70 to 84 as predicted at the B3LYP/6-31G* level

We have also studied $Sc_2S@C_{74}$ [22]. The results show the most favored isomer to be IPR-violating and Sc_2S cluster to be linear inside cage C_{74}:13333. The next two isomers in order of energy lie 11.8 and 11.9 kcal mol^{-1} higher in energy than the first. The cage of the second favored isomer is the only IPR isomer of C_{74}, which itself is open-shell and hence reactive as a neutral cage, but is apparently passivated in the form of $Sc_2S@C_{74}$.

A molecule of stoichiometry $Sc_2S@C_{76}$ has been detected by mass spectrometry, but without further experimental characterization [19]. Our calculations indicate that the isomer of lowest energy is $Sc_2S@C_{76}$:19151, followed by $Sc_2S@C_{76}$:17490, in agreement with recent theoretical results [23]. The third isomer in order of energy is $Sc_2S@C_{76}$:19138. XRD characterization has shown that the C_{76}:19151 cage also encapsulates the Sc_2O cluster to form $Sc_2O@C_{76}$ [24]

For $Sc_2S@C_{78}$, the isomer predicted to have lowest energy has cage C_{78}:24088, a non-IPR fullerene with two pentagon pairs, instead of the well-known IPR cage, C_{78}-24109, which encapsulates two La atoms in the form of $La_2@C_{78}$[25] in relatively high yield. Cage C_{78}:24088 would be only ninth best in terms of the energy of the

tetra-anion C_{78}^{4-}, reminding us that a simple electron-transfer model does not account for the stability of $Sc_2S@C_n$ in every case.

The cage of the most favored $Sc_2S@C_{80}$ is IPR-satisfying C_{80}:31923, which gives the C_{80} tetra-anion of second lowest energy (See S2). The tetra-anion with lowest calculated energy is based on I_h-symmetrical C_{80}:31924, but the triply degenerate LUMO of this cage would tend to indicate acceptance six additional electrons, rather than four that Sc_2S can offer, and it turns out that the isomer of $Sc_2S@C_{80}$ based on the I_h cage has only the third best predicted energy. The cage of the second favored $Sc_2S@C_{80}$ is IPR-satisfying C_{80}-31922, which has recently been shown to be the parent of a geometrically and electronically similar cluster $Sc_2O@C_{80}$ [26] This case demonstrates some of the complexities of the interaction between cage and encapsuland, where predictions of stability based on electronic factors may be in conflict with simple steric matching of size and shape.

In terms of calculated relative energies of the tetra-anion (See S2), C_{82}:39717 should be the best cage for encapsulating a Sc_2S cluster and, in fact, this metallic sulfide fullerene was the first to be reported for any nuclearity [27]. Our calculations predict that $Sc_2S@C_{82}$:39717 and the isomer of lowest calculated energy, $Sc_2S@C_{82}$:39715, are essentially iso-energetic. Although evidently smaller than that of $Sc_2S@C_{82}$:39717, the HOMO-LUMO gap of $Sc_2S@C_{82}$:39715 (1.71 eV) is still relatively large, and this isomer has recently been reported in experiment [28]. Interestingly, non-classical C_{82}^{1h}:155199, the cage of the third best isomer of $Sc_2S@C_{82}$ in our calculations, could serves as a structural bridge between the cages of two experimental isomers of $Sc_2S@C_{82}$, as shown in Fig.2.

For $Sc_2S@C_{84}$, the calculations show that the favored isomer is IPR-$Sc_2S@C_{84}$:51591, sharing a parent cage with $Sc_2C_2@C_{84}$ [29]; the second lowest isomer is non-IPR $Sc_2S@C_{84}$:51383, with predicted high kinetic stability. Our recently reported calculations show that $Sc_2S@C_{84}$:51575 is favored at high temperature (~2800 K); this last isomer can transform to the most favorable isomer $Sc_2S@C_{84}$:51591 via S-W rotation [30].

Geometry optimizations on $Sc_2S@C_n$ with non-classical candidate cages show none that are competitive with classical isomers. The best of the non-classical $Sc_2S@C_n$ isomers with n = 70 to 82 lie respectively 28.5, 32.5, 34.9, 27.8, 34.3, 17.9 and 28.2 kcal mol^{-1} higher than their classical competitors. Thus, isolation of non-classical isomers of these compounds is unlikely.

Cluster effect

I_h-C_{80} is the commonest parent cage for encapsulation of TNT clusters, as demonstrated by numerous experimental observations [4-6]. However, it is not favored for encaging Sc_2S. There are other indications of differences in stability for Sc_2S and TNT clusters. For example, as mentioned above, C_{82}:39718, the cage of the

most favored isomer of $Sc_3N@C_{82}$ [31] is a structural bridge between the cages of two favored candidates, i.e., C_{82}:39717 and C_{82}:39715 for encaging TNT clusters. However, when the encaged cluster is Sc_2S, the bridging isomer is the non-classical isomer C_{82}^{1h}:155199. Significantly, C_2 addition to C_{82}:39715, the favored cage for encaging Sc_2S, can form C_{84}:51383, the parent cage of the second $Sc_2S@C_{84}$; however, C_2 addition to C_{82}:39718, the parent cage of the favored $Sc_3N@C_{82}$ can form C_{84}:51365, the parent cage of EMFs $M_3N@C_{84}$ (M = Tb, Tm and Gd) [32, 33]. These results suggest that the encaged cluster mediates, or even controls, the formation mechanism; this important role could arise from differences in electron-donating capacity (six electrons for TNT cluster and four for the Sc_2S or Sc_2O cluster) and/or different degrees of geometrical match to the cages.

Our recent calculations have shown that the lower symmetry and local deformations associated with introduction of a heptagonal ring favor encapsulation of mixed (and intrinsically less symmetrical) metal nitride clusters [14]. In the present case, however, no non-classical Sc_2S-based EMF is predicted to be competitive with those based on classical cages. Non-classical cages that include one heptagonal face will also tend to have more pentagon adjacencies, almost universally [34] destabilizing in the neutral. As there are two metallic atoms rather than three, it may be easier for them to find suitable internal positions, whether the cage is symmetrical or not, especially as Sc_2S has a low bending force constant [35, 36] and hence is intrinsically more flexible than an M_3N cluster. This may account for the lesser role of non-classical cages in encapsulation of the Sc_2S cluster.

Structural interdependence

The calculations here give a set of favored structures for Sc_2S-based EMFs with eight different cage sizes. As noted above, all predictions for isomers of lowest energy are in agreement with available experimental and theoretical data. Interestingly, there is an evident structural dependence among the parent cages of the low-energy isomers $Sc_2S@C_n$. As shown in Fig. 2, a C_2 unit added to C_{70}:7982 can form C_{72}:10528, and a further C_2 addition forms C_{74}:13333. The corresponding Sc_2S-based EMFs are either those experimentally reported or theoretically predicted to be of lowest energy. A further addition leads to C_{76}:17490, the parent cage of the second favored isomer of $Sc_2S@C_{76}$. Further C_2 addition to C_{76}:17490 can form C_{78}:22010, the parent cage of many TNT fullerenes [37, 38]; another C_2 addition can form C_{80}^{1h}:112912, one Stone-Wales step away from the well-known I_h-symmetric C_{80}:31924, the favored cage for hexavalent (M_3N) clusters. Carrying on the process of C_2 addition can lead to the parent cage (C_{82}:39717) of the first experimentally reported isomer of $Sc_2S@C_{82}$, and the parent cage of the recently reported, and essentially iso-energetic isomer, $Sc_2@C_{82}$:39715 with consecutive S-W rotations. C_2 addition on C_{82}: 39718 can form C_{84}:51365, the parent of $M_3N@C_{84}$ (M=Tb, Tm and Gd) [32, 33].

In another part of the map, the unique IPR isomer of C_{70}, i.e., C_{70}:8149, has a tetra-anion energy that makes it

the favored candidate for encaging a cluster that would donate four electrons. C_2 addition to C_{70}:8149 can lead to C_{72}:11188, fifth best in terms of its tetra-anion energy. In turn, C_{72}:11188 can isomerize into a non-classical isomer C_{72}^{1h}-29907 with two pairs of fused pentagons, which can form C_{74}:14246 via directly C_2 addition. C_{74}:14246 can form C_{76}:19138 and C_{78}:24088 via successive C_2 addition. Interestingly, C_2 addition on the parent cage of most favored $Sc_2S@C_{80}$:31923 can lead to C_{82}:39663, which has recently been proved to be the parent of $Gd_3N@C_{82}$[39, 40], this cage is an S-W rotation away from the parent cage of the most favored isomer $Sc_2S@C_{82}$:39715.

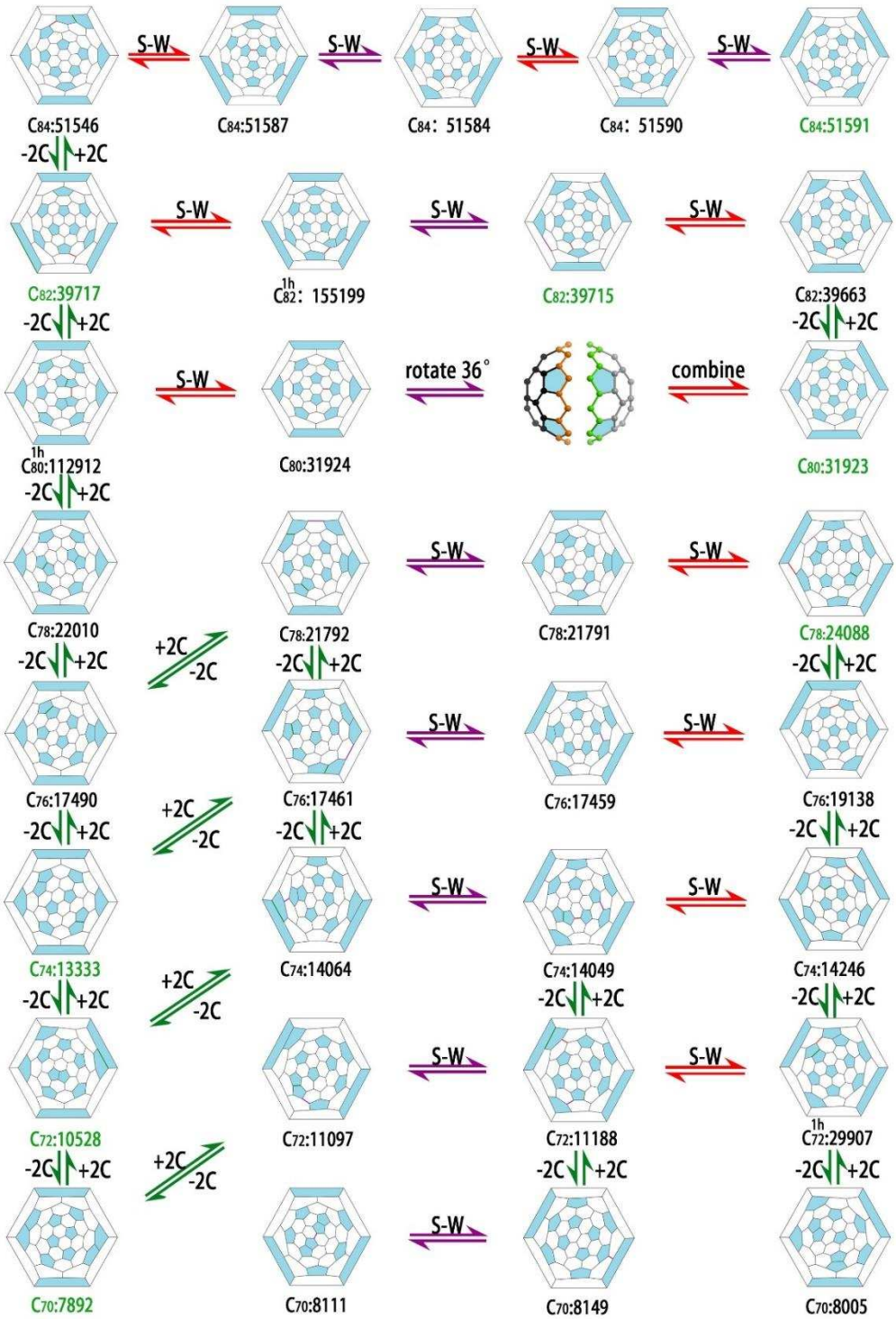

Fig. 2 The structural web (atlas) of $Sc_2S@C_n$ isomers. Arrows in red and purple indicate that a Stone-Wales isomerization can interconvert two isomers; colored edges indicate the atoms undergoing a Stone-Wales rotation.

Exploration of the details encoded in the figure show that the vertical and diagonal connections in the map provide a route for expansion/shrinkage of all eight parent cages of low-energy isomers from $Sc_2S@C_{70}$ to $Sc_2S@C_{84}$.

C_{70}:7892, the parent of the most favored isomer of $Sc_2S@C_{70}$ can transform into C_{70}:8111 via a C_2 extrusion (C_{68}:6094) and C_2 insertion, and then isomerize into C_{70}:8149; C_{68}:6094 has been captured as $C_{68}Cl_8$ by in situ chlorination in the gas phase during radio-frequency synthesis [41] and theoretically predicted to be the parent of Sc_2O_2 [42]. C_{72}:10528, the parent of the most favored isomer of $Sc_2S@C_{72}$, has a transformation to C_{72}:11188, one of the molecules of lowest energy for this stoichiometry. The isomer of lowest energy $Sc_2S@C_{74}$:13333, can transform into the second-best $Sc_2S@C_{74}$:14246 as shown in Fig.2. C_{76}:14790 can transform into C_{76}:19138, the second best cage for both tetra-valent and di-valent clusters, according to the relative energies of the anions. In fact, C_{76}:19138 has been shown to encage divalent Sm [43]. C_{76}:19142 can transform into C_{76}-19151 via an S-W rotation (not shown), the parent cage of lowest energy for $Sc_2S@C_{76}$. C_{78}:24099 can transform into C_{78}:24109 via an S-W rotation, the isomer most favored for encaging Sc_2O [44]. C_{78}-22010, the most favored cage for the large metallic cluster Gd_3N [37] can transform into C_{78}-24088, the most favored cage for Sc_2S. Interestingly, C_{70}:7892, C_{72}:10528, C_{74}:13333, C_{76}:17490 and C_{78}:22010 all have similar transformations (extrusion/insertion and then isomerization) to their low energy counterparts. The I_h-C_{80} cage can transfer into D_{5h}-C_{80} via three kinds of path; the first is by growth, shrinkage and isomerization, the second is by shrinkage, growth and isomerization; the third path (at least in in a formal mathematical sense) is by a 36º rotation around a C_5 axis of one half of I_h-C_{80} against the other. C_{82}-39717 can isomerize into C_{82}-39715, the parent cage of a recently experimentally reported isomer $Sc_2S@C_{82}$ [28] via a non-classical bridge cage, C_{82}^{1h}-155199. Successive S-W rotations can transfer C_{84}:51546 into the most favored neutral cage C_{84}:51590, and the parent cage of lowest energy $Sc_2S@C_{84}$, C_{84}:51591.

In summary, favored cages can grow or shrink in the vertical direction on the map, or isomerize in the horizontal direction into other favored cages. Horizontal connections in the map typically provide a possible route from one favored isomer to another of $Sc_2S@C_n$. These include the global rotation of one hemisphere against another, which would have a high energy barrier for a pre-formed cluster, but for a mechanism involving combination of fragments would be a low-energy process. The parent fullerene cages and the low-energy Sc_2S-based EMFs form a web of complex genealogical relationships. Many of the cages in the near region of this map are favored for encapsulation of other types of mono-metallic, di-metallic or metallic clusters, all

demonstrating common stabilizing substructures and motifs.

Formation mechanisms

The calculations of optimal structures demonstrate that C_2 insertion/extrusion is not only a topological requirement but also a possible bridge for growth of favored Sc_2S-based EMFs, connecting isomers of low energy. As the most common metallic atom(s) or clusters would have extremely high barriers to insertion through a pentagon or hexagon of fullerene, it seems likely that the Sc_2S cluster would be encaged early in the process inside a fullerene (or fullerene-like) cage that could continue to grow or shrink via C_2 insertion or extrusion, eventually forming a stable EMF. D_{3h}-C_{78}, I_h-C_{80}, D_{5h}-C_{80}, C_{2V}-C_{82}, C_{3V}-C_{82} and D_{2d}-C_{84} are all IPR-satisfying and comprise the set of parent cages of most EMFs, but they cannot be formed by direct C_2 insertion into a lower IPR fullerene, and so at least one S-W isomerization step is necessary. This remains true in models of growth from smaller clusters, since even if an IPR-satisfying cage of C_{n+2} can be formed directly via C_2 insertion into the heptagon of a non-classical isomer, an S-W isomerization would be needed for initial transformation from a classical isomer.

Molecular dynamics simulations have shown that hot giant fullerenes can lose or gain carbon in high temperature conditions [45]. This existence of a structural web such as shown in Fig. 2 suggests that, irrespective of the formation mechanism of $Sc_2S@C_n$,, there are generally many $Sc_2S@C_n$ species with different sizes, since any as-formed $Sc_2S@C_n$ can produce other metallic sulfide fullerenes via top-down [46] or bottom-up [47] paths and S-W isomerization. Experiment shows that there are always many $Sc_2S@C_n$ species in the soot [17, 19a, 48], and multiple species with different metallic atoms or clusters encaged inside different fullerene cages are produced under the same reaction conditions. For example, a mixture of several $Sc_2O@C_n$, multiple $Sc_2C_2@C_n$, and even $Sc_3N@C_{80}$ species are found in soot produced under conditions designed to yield $Sc_2O@C_n$ by introducing CO_2 as the oxygen source during the arcing process [21]; a mixture of $Sc_2S@C_n$ and $Sc_2C_2@C_{80}$ isomers is found in soot in a conventional Krätschmer-Huffman reactor for producing metallic sulfide fullerenes under an atmosphere of SO_2 [19]. The difficulty in isolating a particular EMF is mainly a result of the diversity of EMFs in reaction mixtures.

Recently, Wang et al. identified four key structural motifs which govern the relative energies of anions of classical fullerene cages and thus can be used to search for suitable cages in endohedral metallofullerenes [49]. This is a significant finding, but more rules would be desirable since these motifs are compatible with many structural isomers. Our study helps to refine the predictive picture by setting the mass of experimental results scattered in the literature into the context of a relatively small family of low-energy isomers.

A further remark can be made. We have considered fullerenes encapsulating metallic sulfide clusters from the point of view of their structural interdependence. However, our main findings are likely to be valid for Sc_2C_2 and Sc_2O in fullerene cages. The carbide Sc_2C_2 has similar electronic properties to Sc_2S, and Sc_2O and Sc_2S are similar in both electronic and geometrical requirements. Thus, the present calculations may have implications for a larger family of EMFs beyond compounds of Sc_2S.

4. Conclusion

Systematic DFT calculations demonstrate that there is a close structural interdependence amongst the favored isomers of $Sc_2S@C_n$ with size from C_{70} to C_{84}, and that one-heptagon non-classical $Sc_2S@C_n$ are generally much less competitive relative to classical cages in terms of total energetics. This is quite unlike the situation that we found for tri-metallic nitride fullerenes. These results indicate that formation of $Sc_2S@C_n$ and other EMFs is guided by the encaged clusters, and suggests a similar formation route in that cages featuring as preferred have closely related structures.

As a whole, the stability of EMFs is determined by two main factors: one is electron transfer and the other is effect of size. Calculations show that many of the lowest energy isomers of $Sc_2O@C_n$ share the same cages with $Sc_2S@C_n$ apart from the cases with n=74, 78 and 84. Since both Sc_2O and Sc_2S tend to donate 4 electrons to a fullerene cage, they tend to select the same isomer as host cage and these results indicate that electron transfer interactions play a vital role. Of course, the cluster sizes are different, and rankings are evidently different when comparing structures involving a series of cages of size C_n (when the sizes and shapes of both cages and the encaged clusters play an important role).

Acknowledgement

The authors thank Gunnar Brinkmann (Ghent University) for cross-checking completeness of the face-spiral construction for the non-classical cages discussed here.

References

1. H. Shinohara, *Rep. Prog. Phys*. **2000**, *63*, 843-892.
2. A. Rodríguez-Fortea, A. L. Balch, J. M. Poblet, *Chem. Soc. Rev*. **2011**, *40*, 3551-3563.
3. Y. Chai, T. Guo, C. Jin, R. E. Haufler, L. P. F. Chibante, J. Fure, L. Wang, J. M. Alford, R. E. Smalley, *J. Phys. Chem*. **1991**, *95*, 7564-7568.
4. A. A. Popov, S. Yang, L. Dunsch, *Chem. Rev*. **2013**, *113*, 5989-6113.

5. J. Zhang, S. Stevenson, H. C. Dorn, *Acc. Chem. Res*. **2013**, *46*, 1548-1557.
6. T. Wang, C. Wang, *Acc. Chem. Res*., **2014**, *47*, 450-458.
7. J. S. Dang, W. W. Wang, J. J. Zheng, X. Zhao, E. Osawa, S. Nagase, *J. Phys. Chem. C*, **2012**, *116*, 16233-16239.
8. H. W. Kroto, *Nature*, **1987**, *329*, 529-531.
9. Q. Deng, T. Heine, S. Irle, A. A. Popov, *Nanoscale*, **2016**, *8*, 3796-3808.
10. Y. Zhang, K. B. Ghiassi, Q. Deng, N. A. Samoylova, M. M. Olmstead, A. L. Balch, A. A. Popov, *Angew. Chem. Int. Ed*. **2015**, *54*, 495-499.
11. Y. Z. Tan, R. T. Chen, Z. J. Liao, J. Li, F. Zhu, X. Lu, S. Y. Xie, J. Li, R. B. Huang, L. S. Zheng, *Nat. Commun*. **2011**, *2*, 1-6.
12. E. Hernandez, P. Ordejon, H. Terrones, *Phys. Rev. B*., **2001**, *63*, 193403.
13. a) W. W. Wang, J. S. Dang, J. J. Zheng, X. Zhao, *J. Phys. Chem. C*, **2012**,*116*, 17288-17293; b) W. W. Wang, J. S. Dang, J. J. Zheng, X. Zhao, S. Nagase, *J. Phys. Chem. C*, **2013**, *117*, 2349-2357.
14. L. H. Gan, D. Lei, P. W. Fowler, *J. Comput. Chem*. **2016**, *37*, 1907-1913.
15. P. W. Fowler, D. E. Manolopoulos, An Atlas of Fullerenes; Clarendon Press, Oxford, **1995**.
16. M. J. Frisch, G. W. Trucks, H. B. Schlegel, G. E. Scuseria, M. A. Robb, J. R. Cheeseman, G. Scalmani, V. Barone, B. Mennucci, G. A. Petersson, H. Nakatsuji, M. Caricato, X. Li, H. P. Hratchian, A. F. Izmaylov, J. Bloino, G. Zheng, J. L. Sonnenberg, M. Hada, M. Ehara, K. Toyota, R. Fukuda, J. Hasegawa, M. Ishida, T. Nakajima, Y. Honda, O. Kitao, H. Nakai, T. Vreven, J. A. Montgomery, Jr. J. E. Peralta, F. Ogliaro, M. Bearpark, J. J. Heyd, E. Brothers, K. N. Kudin, V. N. Staroverov, R. Kobayashi, J. Normand, K. Raghavachari, A. Rendell, J. C. Burant, S. S. Iyengar, J. Tomasi, M. Cossi, N. Rega, J. M. Millam, M. Klene, J. E. Knox, J. B. Cross, V. Bakken, C. Adamo, J. Jaramillo, R. Gomperts, R. E. Stratmann, O. Yazyev, A. J. Austin, R. Cammi, C. Pomelli, J. W. Ochterski, R. L. Martin, K. Morokuma, V. G. Zakrzewski, G. A. Voth, P. Salvador, J. J. Dannenberg, S. Dapprich, A. D. Daniels, O. Farkas, J. B. Foresman, J. V. Ortiz, J. Cioslowski, and D. J. Fox. Gaussian 09; Revision A. 02 Gaussian Inc.: Pittsburgh, PA, **2009**.
17. N. Chen, M. Mulet-Gas, Y. Y. Li, R. E. Stene, C. W. Atherton, A. Rodríguez-Fortea, J. M. Poblet, L. Echegoyen, *Chem. Sci.*, **2013**, *4*, 180-186.
18. L. Feng, M. Zhang, Y. Hao, Q. Tang, N. Chen, Z. Slanina, F. Uhlík, *Dalton Trans*., **2016**,*45*,8142-8148.
19. N. Chen, C. M. Beavers, M. Mulet-Gas, A. Rodríguez-Fortea, E. J. Munoz, Y. Y. Li, M. M. Olmstead, A. L. Balch, J. M. Poblet, L. Echegoyen, *J. Am. Chem. Soc.* **2012**, *134*, 7851-7860; L.-J. Wang, R.-L. Zhong, S.-L. Sun, H.-L. Xu, X.-M. Pan and Z.-M. Su, *Dalton Trans*., **2014**, *43*, 9655.
20. Y. Feng, T. Wang, J. Wu, L. Feng, J. Xiang, Y. Ma, Z. Zhang, L. Jiang, C. Shu, C. Wang, *Nanoscale*, **2013**, *5*, 6704-6707.
21. M. Zhang, Y. Hao, X. Li, L. Feng, T. Yang, Y. Wan, N. Chen, Z. Slanina, F. Uhlík, H. Cong, *J. Phys. Chem. C.*, **2014**, *118*, 28883-28889.
22. L. H. Gan, Q. Chang, C. Zhao, C. R. Wang, *Chem. Phys. Lett*. **2013**, *570*,121-124.
23. P. Zhao, T. Yang, Y. J. Guo, J. S. Dang, X. Zhao, S. Nagase, *J. Comput. Chem.* **2014**, *35*, 1657-1663.
24. T. Yang, Y. Hao, L. Abella, Q. Tang, X. Li, Y. Wan, A. Rodríguez-Fortea, J. M. Poblet, L. Feng, N. Chen, *Chem. Eur. J*. **2015**, *21*, 11110-11117.
25. B. Cao, T. Wakahara, T. Tsuchiya, M. Kondo, Y. Maeda, G. M. A. Rahman, T. Akasaka, K. Kobayashi, S. Nagase, K.

Yamamoto, *J. Am. Chem. Soc*. **2004**, *126*, 9164-9165.

26. Q. Tang, L. Abella, Y. Hao, X. Li, Y. Wan, A. Rodríguez-Fortea, J. M. Poblet, L. Feng, N. Chen, *Inorg. Chem*., **2015**, *54*, 9845-9852.
27. L. Dunsch, S. Yang, L. Zhang, A. Svitova, S. Oswald, A. A. Popov, *J. Am. Chem. Soc*. **2010**, *132*, 5413-5421.
28. B. Q. Mercado, N. Chen, A. Rodríguez-Fortea, M. A. Mackey, S. Stevenson, L. Echegoyen, J. M. Poblet, M. M. Olmstead, A. L. Balch, *J. Am. Chem. Soc*. **2011**, *133*, 6752-6760.
29. C. R. Wang, T. Kai, T. Tomiyama, T. Yoshida, Y. Kobayashi, E. Nishibori, M. Takata, M. Sakata, H. Shinohara, *Angew. Chem. Int. Ed*., **2001**, *40*, 397-399.
30. C. Zhao, D. Lei, L. H. Gan, Z. X. Zhang, C. R. Wang, *ChemPhysChem,* **2014**, *15*, 2780-2784.
31. T. Wei, S. Wang, F. Liu, Y. Tan, X. Zhu, S. Xie, S. Yang, *J. Am. Chem. Soc*. **2015**, *137*, 3119-3123.
32. C. M. Beavers, T. Zuo, J. C. Duchamp, K. Harich, H. C. Dorn, M. M. Olmstead, A. L. Balch, *J. Am. Chem. Soc*. **2006**, *128*, 11352-11353.
33. T. Zuo, K. Walker, M. M. Olmstead, F. Melin, B. C. Holloway, L. Echegoyen, H. C. Dorn, M. N. Chaur, C. J. Chancellor, C. M. Beavers, A. L. Balch, A. J. Athans, *Chem. Commun*., **2008**,1067-1069.
34. A. S. Matias, R. W. A. Havenith, M. Alcami, A. Ceulemans, *Phys. Chem. Chem. Phys*. **2016**, *18*, 11653-11660.
35. Q. Deng, A. A. Popov, *J. Am. Chem. Soc*. **2014**, *136*, 4257-4264.
36. Q. Tang, L. Abella, Y. Hao, X. Li, Y. Wan, A. Rodríguez-Fortea, J. M. Poblet, L. Feng, N. Chen, *Inorg. Chem*. **2016**, *55*, 1926-1933.
37. C. M. Beavers, M. N. Chaur, M. M. Oimstead, L. Echegoyen, A. L. Balch, *J. Am. Chem*. *Soc*. **2009**, *131*, 11519 -11524.
38. A. A. Popov, M. Krause, S. Yang, J. Wong, L. Dunsch, *J. Phys. Chem. B*, **2007**, *111*,3363-3369.
39. M. Mulet-Gas, A. Rodríguez-Fortea, L. Echegoyen, J. M. Poblet, *Inorg. Chem*, **2013**, *52*, 1954-1959.
40. B. Q. Mercado, C. M. Beavers, M. M. Olmstead, M. N. Chaur, K. Walker, B. C. Holloway, L. Echegoyen, and A. L. Balch, *J. Am. Chem. Soc*. **2008**, *130*, 7854-7855.
41. P. Zhao, M. Y. Li, Y. J. Guo, R. S. Zhao, X. Zhao, *Inorg. Chem*. **2016**, *55*, 2220-2226.
42. N. Chen, M. N. Chaur, C. Moore, J. R. Pinzón, R. Valencia, A. Rodríguez-Fortea, J. M. Poblet, L. Echegoyen, *Chem. Commun*., **2010**, 4818-4820.
43. Y. Hao, L. Feng, W. Xu, Z. Gu, Z. Hu, Z. Shi, Z. Slanina, F. Uhlík, *Inorg. Chem*., **2015**, *54*, 4243-4248.
44. B. Saha, S. Irle, Keiji, Morokuma, *J. Phys. Chem. C*., **2011**, *115*, 22707-22716.
45. J. Zhang, F. L. Bowles , D. W. Bearden, W. K. Ray, T. Fuhrer, Y. Ye, C. Dixon, K. Harich, R. F. Helm, M. M. Olmstead, A. L. Balsh, H. C. Dorn, *Nature Chem.*, **2013**, 5, 880-885.
46. P. W. Dunk, M. Mulet-Gas, Y. Nakanishi, N. K. Kaiser, A. Rodríguez-Fortea, H. Shinohara, J. M. Poblet, A. G. Marshall, H. W. Kroto, *Nature Comm*. **2014**, 5, 1-8.
47. Y. Wang, S. Díaz-Tendero, F. Martín, and M. Alcamí**,** *J. Am. Chem. Soc*. **2016**, *138*, 1551-1560.
48. B. Q. Mercado, C. M. Beavers, M. M. Olmstead, M. N. Chaur, K. Walker, B. C. Holloway, L. Echegoyen, and A. L. Balch, *J. Am. Chem. Soc*. **2008**, *130*, 7854-7855.